BIOCHEMISTRY
including biophysical chemistry & molecular biology
Article

Biochemistry **2009,** *48,* 12233–12241 12233
DOI: 10.1021/bi901181z

Characterization of an AM404 Analogue, *N*-(3-Hydroxyphenyl)arachidonoylamide, as a Substrate and Inactivator of Prostaglandin Endoperoxide Synthase[†]

Melissa V. Turman,[‡] Philip J. Kingsley, and Lawrence J. Marnett*

A. B. Hancock, Jr., Memorial Laboratory for Cancer Research, Departments of Biochemistry, Chemistry, and Pharmacology, Vanderbilt Institute of Chemical Biology, Center in Molecular Toxicology, and Vanderbilt-Ingram Cancer Center, Vanderbilt University School of Medicine, Nashville, Tennessee 37232. [‡]Current address: Immune Disease Institute and Department of Pathology, Harvard Medical School, Boston, MA 02115.

Received July 10, 2009; Revised Manuscript Received November 17, 2009

ABSTRACT: *N*-(4-Hydroxyphenyl)arachidonoylamide (AM404) is an inhibitor of endocannabinoid inactivation that has been used in cellular and animal studies. AM404 is a derivative of arachidonic acid and has been reported to inhibit arachidonate oxygenation by prostaglandin endoperoxide synthase-1 and -2 (PGHS-1 and -2, respectively). While examining the structural requirements for inhibition of PGHS, we discovered that the *meta* isomer of AM404, *N*-(3-hydroxyphenyl)arachidonoylamide (3-HPAA), is a substrate for purified PGHS. PGHS-2 efficiently oxygenated 3-HPAA to prostaglandin and hydroxyeicosatetraenoate products. No oxidation of the phenolamide moiety was observed. 3-HPAA appeared to be converted by PGHS-1 in a similar manner; however, conversion was less efficient than that by PGHS-2. PGHS-2 was selectively, dose-dependently, and irreversibly inactivated in the presence of 3-HPAA. Complete inactivation of PGHS-2 was achieved with 10 μM 3-HPAA. Preliminary characterization revealed that 3-HPAA inactivation did not result from covalent modification of PGHS-2 or damage to the heme moiety. These studies provide additional insight into the structural requirements for substrate metabolism and inactivation of PGHS and report the first metabolism-dependent, selective inactivator of PGHS-2.

Prostaglandin endoperoxide synthase (PGHS)[1] is involved in many physiological and pathophysiological functions. Prostaglandin H_2 (PGH_2) is an end product of the PGHS reaction and serves as the precursor for prostaglandins, prostacyclin, and thromboxane, which mediate processes such as inflammation, platelet aggregation, and cell proliferation, among others (*1*, *2*). PGHS catalyzes the removal of a bis-allylic hydrogen from arachidonate, which allows sequential incorporation of two molecules of oxygen into the fatty acid substrate to yield the hydroperoxyendoperoxide, prostaglandin G_2 (PGG_2) (Figure 1A). The hydroperoxide of PGG_2 is subsequently reduced at a separate peroxidase active site of the protein to yield the hydroxyendoperoxide, PGH_2. Most mammals express two functional isoforms of PGHS, designated PGHS-1 and PGHS-2 (*3*−*5*). The expression profiles and biological functions of the isoforms differ (*6*), although the proteins are homologous in sequence and structure (*3*−*5*, *7*).

Structural and functional studies reveal that fatty acid substrates bind to PGHS in an inverted L-shaped conformation (Figure 1B) (*8*−*11*). This conformation is required to yield the appropriate product stereochemistry (*12*). Fatty acids utilize ionic and/or hydrogen bonding to active site residues Arg-120 and Tyr-355 to stabilize binding (*9*). Arg-120 is required for high-affinity binding to PGHS-1 but not PGHS-2 (*13*). In PGHS-2, the presence of valine at positions 434 and 523, which are both occupied by isoleucine in PGHS-1, increases the active site volume and allows ligands access to an additional hydrophilic interaction at Arg-513 (*7*, *14*). These key structural differences allow PGHS-2 to metabolize a wider range of substrates than PGHS-1 (*15*−*17*). PGHS-2-selective substrates include the endocannabinoids 2-arachidonoylglycerol and arachidonoylethanolamide, as well as arachidonoylamides of amino acids (glycine, alanine, and γ-aminobutyric acid). However, PGHS-2 does not efficiently metabolize bulkier aromatic conjugates of arachidonate such as *N*-arachidonoyldopamine or its *O*-desmethyl analogue.

AM404 (Figure 1C) is a phenolamide conjugate of arachidonic acid that can be generated in vivo from acetaminophen or *p*-aminophenol (*18*). It was first described as an inhibitor of cellular endocannabinoid uptake (*19*) and has been used as an alternative to cannabinoid receptor agonists in animal studies of the physiology of endocannabinoids (*20*−*22*). However, AM404 acts at multiple targets. It inhibits fatty acid amide hydrolase (*23*), the key enzyme regulating arachidonoylethanolamide levels, activates transient receptor potential vanilloid receptor 1 (*24*), and inhibits both isoforms of PGHS (*18*). In an effort to understand determinants of binding and metabolism of arachidonoylamides,

[†]This work was supported by National Institutes of Health Research Grant CA89450 (L.J.M.) and a training grant to M.V.T. (ES07028). M.V.T. is the recipient of a Ruth L. Kirschstein National Research Service Award (DA02014) from the National Institutes of Health/National Institute of Drug Abuse and a fellowship from the Vanderbilt Institute of Chemical Biology.

*To whom correspondence should be addressed: Department of Biochemistry, Vanderbilt University School of Medicine, Nashville, TN 37232-0146. Phone: (615) 343-7329. Fax: (615) 343-7534. E-mail: larry.marnett@vanderbilt.edu.

[1]Abbreviations: PGHS, prostaglandin endoperoxide synthase; PG, prostaglandin; AM404, *N*-(4-hydroxyphenyl)arachidonoylamide; 3-HPAA, *N*-(3-hydroxyphenyl)arachidonoylamide; X-PA, conjugate to the phenolamide group; LC, liquid chromatography; MS, mass spectrometry; CID, collision-induced dissociation; mu, mass unit; Ag^+CIS-MS, silver ion coordination ion spray mass spectrometry; HHT, 12-hydroxyheptadecatrienoate; HETE, hydroxyeicosatetraenoate.

Published on Web 11/20/2009

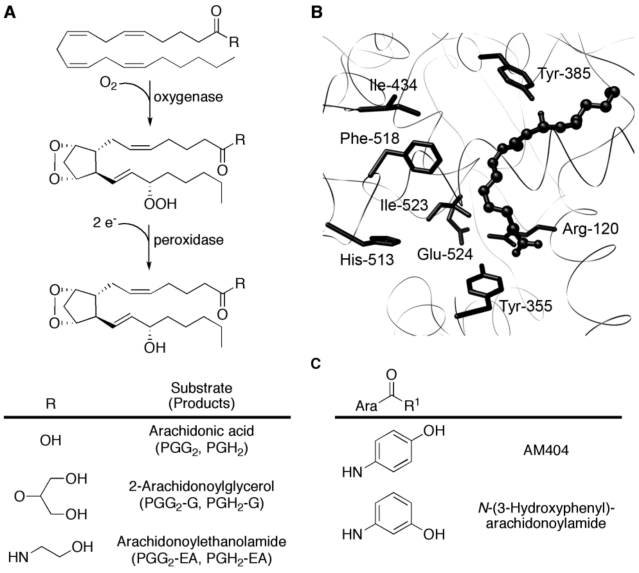

FIGURE 1: (A) Conversion of arachidonoyl-derived substrates by PGHS. Two molecules of molecular oxygen are incorporated at the oxygenase site of PGHS to yield PGG_2. In vitro, the peroxidase of PGHS reduces the hydroperoxide to form PGH_2. PGHS-2 catalyzes identical reactions with 2-arachidonoylglycerol and arachidonoylethanolamide. (B) Structure of arachidonic acid in its productive conformation bound to PGHS-1. Arachidonate (ball and stick) binds to PGHS in an inverted L-shaped conformation, positioning the *pro-S* hydrogen at C-13 for abstraction by Tyr-385. The carboxylate binds at the constriction site created by Arg-120, Tyr-355, and Glu-524. Substitutions at residues 434, 513, and 523 allow PGHS-2 to bind and oxygenate acyl amides and esters of arachidonate. (C) Chemical structures of arachidonoylphenolamides.

we synthesized a small series of substituted phenylarachidonoylamides. This led to the discovery that the *meta* isomer of AM404, *N*-(3-hydroxyphenyl)arachidonoylamide (3-HPAA), is oxygenated by PGHS and leads to enzyme inactivation. Thus, 3-HPAA appears to be a mechanism-based inactivator of PGHS, with selectivity for PGHS-2.

EXPERIMENTAL PROCEDURES

Materials. Arachidonic acid was purchased from NuChek Preps (Elysian, MN). AM404 was purchased from Cayman Chemical (Ann Arbor, MI). Ovine PGHS-1 was purified from ram seminal vesicles (Oxford Biomedical Research, Oxford, MI) by ion exchange and gel filtration, as previously described (*25*).

Expression and Purification of PGHS-2. Murine PGHS-2 containing a C-terminal 12-histidine tag was expressed in *Spodoptera frugiperda* 21 insect cells (Invitrogen, Carlsbad, CA) from recombinant baculovirus generated from the BD Baculogold pVL1393 transfer vector (BD Biosciences, San Jose, CA). Cell pellets were stored at −20 °C until purification. Cells (approximately 30 g of wet weight) were resuspended in 10 volumes/wet weight lysis buffer [25 mM Tris-HCl and 250 mM sucrose (pH 8.0)] while being stirred. The pellet was collected by centrifugation at 10000*g* and resuspended in the same volume of lysis buffer. CHAPS was added dropwise to a final concentration of 1% (v/v) from an 11% stock solution, and the solution was stirred at 4 °C for 30 min. The supernatant was collected after centrifugation at 48000*g* for 20 min. Imidazole was added to the supernatant to a final concentration of 20 mM, and the supernatant was mixed overnight at 4 °C with 10 mL of NiNTA Superflow resin (Qiagen, Valencia, CA) that had been equilibrated with 25 mM Tris-HCl and 20 mM imidazole (pH 8.0) with 0.4% CHAPS. The slurry was transferred to a gravity flow column and washed with 3 column volumes (CV) of 25 mM Tris-HCl and 20 mM imidazole (pH 8.0) with 0.4% CHAPS. The concentration of imidazole was increased linearly from 20 to 500 mM over 30 CV. Pooled fractions were concentrated and dialyzed overnight at 4 °C against 20 mM Tris-HCl and 150 mM NaCl (pH 8.0) with 0.4% CHAPS. PGHS-2 was greater than 95% pure as determined by SDS−PAGE with BioSafe Coomassie stain (Invitrogen), and the specific activity determined by oxygen uptake assay was 14 μmol of arachidonate per minute per milligram of protein.

Synthesis of 3-HPAA. A solution of pyridine containing 1 equiv of 3-aminophenol (0.12 mmol, 13 mg) was cooled to 10 °C and treated with 1 equiv of arachidonoylchloride (0.12 mmol, 40 mg) dissolved in pyridine. The reaction mixture was stirred at room temperature for approximately 2 h, diluted with EtOAc, and washed with water three times. The organic layer was dried over magnesium sulfate, filtered, and dried in vacuo. 3-HPAA was obtained by silica gel chromatography (1:4 EtOAc/hexanes) as a light yellow oil (48%): ^{1}H NMR ($CDCl_3$) δ 0.87 (t, 3H, J = 6.8 Hz, CH_2), 1.30 (m, 7H, 3 × CH_2 + MeOH), 1.83 (quintet, 2H, J = 7.5 Hz, CH_2), 2.05 (quartet, 2H, J = 6.8 Hz, CH_2), 2.17 (quartet, 2H, J = 6.8 Hz, CH_2), 2.39 (t, 2H, J = 7.6 Hz), 2.80 (m, 6H, 3 × CH_2), 5.39 (m, 8H, 8 × CH), 6.48 (dd, 1H, J_a = 7.9 Hz, J_b = 1.1 Hz, ArH), 6.65 (dd, 1H, J_a = 8.1 Hz, J_b = 1.8 Hz, ArH), 7.14 (t, 1H, J = 8.0 Hz, ArH), 7.27 (s, 1H, NH), 7.97 (m, 1H, J = 2.0 Hz, ArH); ESI-MS m/z [M + Na^+] 418.3.

Synthesis of PGE_2-Phenolamide. To prepare a synthetic standard of the *m*-phenolamide of PGE_2 (PGE_2-PA), 1 equiv of PGE_2 (49 μmol, 17.4 mg), 1.5 equiv of 3-aminophenol (73 μmol, 8.0 mg), 2.3 equiv of diisopropylethyl amine (114 μmol, 14.7 mg), and 2.4 equiv of *O*-(7-azabenzotriazol-1-yl)-*N*,*N*,*N*′,*N*′-tetramethyluronium hexafluorophosphate (HATU) were mixed in anhydrous ACN overnight. PGE_2-PA was purified by preparative normal phase thin layer chromatography (4:1 EtOAc/hexanes with 0.1% acetic acid; R_f = 0.49): ^{1}H NMR (MeOD) δ 0.89 (t, 3H, J = 6.6 Hz, CH_3), 1.40 (m, 8H, 4 × CH_2), 1.73 (quintet, 2H, J = 7.6 Hz, CH_2), 2.11 (m, 4H, 2 × CH_2), 2.34 (m, 5H, 2 × CH_2 + CH), 2.67 (dd, 1H, J_a = 7.4 Hz, J_b = 18 Hz, CH), 4.03 (m, 2H, 2 × CH), 5.34 (m, 1H, CH), 5.44 (m, 1H, CH), 5.59 (m, 2H, 2 × CH), 6.50 (d, 1H, J = 8.0 Hz, ArH), 6.92 (d, 1H, J = 7.6 Hz, ArH), 7.07 (t, 1H, J = 8.0 Hz, ArH), 7.15 (s, 1H, ArH); ESI-MS m/z [M + H]$^+$ 444.2, [M + NH_4]$^+$ 461.2, [M + Na]$^+$ 466.2.

Synthesis of [1-^{14}C]-N-(3-Hydroxyphenyl)eicosa-5,8,11,14-tetraenamide ([^{14}C]-3-HPAA). [1-^{14}C]Arachidonic acid supplied in ethanol (American Radiolabeled Chemicals, Inc., St. Louis, MO) was dried in vacuo. A mixture containing 1 equiv of [1-^{14}C]arachidonic acid (9.1 μmol, 2.79 mg), 1.5 equiv of 3-aminophenol (13.6 μmol, 1.5 mg), 1.25 equiv of HATU (11.4 μmol, 4.3 mg), and 3 equiv of triethylamine (27.3 μmol, 2.7 mg) was dissolved in anhydrous ACN and allowed to react overnight. Separation of the reaction mixture was achieved on system C on an Agilent Zorbax Rx-SIL column (0.46 cm × 25 cm, 5 μm). The mobile phase consisted of IPA and cyclohexane. The flow rate was held constant at 1 mL/min. The IPA concentration was held at 5% for 5 min, increased to 50% over 1 min, and held at 50% for 7 min prior to reequilibration. Analytes were detected by UV absorption at 245 and 280 nm and by β-RAM. Under these conditions, [^{14}C]-3-HPAA eluted at 4.6 min. After reaction for 19 h, approximately 70% [1-^{14}C]arachidonic acid had been converted to [^{14}C]-3-HPAA

and an additional 10% had been converted to a secondary product. The reaction mixture was dried in vacuo and resuspended in 5% isopropanol (IPA) in cyclohexane with heating. [^{14}C]-3-HPAA was purified by normal phase liquid chromatography (LC) as described on system C (see below), bypassing the β-RAM. Fractions were pooled and dried in vacuo, resuspended in ethanol, and stored at −20 °C. The final product was obtained in 20% yield at >99% purity by UV detection at 245 and 280 nm and by β-RAM detection.

Kinetics of 3-HPAA Oxidation by PGHS. The metabolism of substrates was characterized by oxygen uptake as previously described (*26*). To determine Michaelis−Menten kinetic parameters, the concentration of substrate was varied (1 to 50 μM), and rates of metabolism were determined by an O_2 uptake assay. Maximal rates were converted from volts per second to micromolar O_2 per second using the calibration constant determined by ferricyanide-catalyzed oxidation of phenylhydrazine (*27*). Converted rates were plotted versus substrate concentration and fit by nonlinear regression (Prism 4.0, GraphPad Software, San Diego, CA) to determine v_{max} and K_m.

Enzyme Inactivation following 3-HPAA Metabolism. To characterize the extent of enzyme inactivation associated with 3-HPAA metabolism, PGHS-1 or PGHS-2 was incubated with 25 μM 3-HPAA. When oxygen uptake was complete, arachidonic acid (25 μM) was added, and the maximal rate was determined as described above and normalized to the DMSO control. The concentration dependence of PGHS-2 inactivation was analyzed in a similar manner with varying concentrations of 3-HPAA (from 10 nM to 25 μM).

Reversibility of 3-HPAA-Dependent Inactivation of PGHS. PGHS (7.5 μM) was reconstituted with 2.5 equiv of heme in reaction buffer. Reconstituted protein was incubated with DMSO or 1.5 mM 3-HPAA at 37 °C for 90 s and then cooled to 4 °C. Aliquots were assayed for activity using the oxygen uptake system. Remaining samples were transferred to centrifugal filter devices (molecular mass cutoff of 30000 kDa), and excess inhibitor was removed by three successive buffer exchanges. Following buffer exchange, an additional 2.5 equiv of heme was added to the protein, and aliquots of each sample were again assayed by oxygen uptake. Activity was normalized to the DMSO control.

Liquid Chromatography. Multiple LC systems and conditions were utilized, dependent upon the application. The systems and chromatography conditions are described here. System A consisted of a Waters 717plus autosampler and a Waters 1525 binary HPLC pump in line with a Waters 2996 photodiode array detector. System B consisted of a Waters Alliance 2695 separation module equipped with a Waters 2487 dual-wavelength absorbance detector and a Sedere Sedex 75 evaporative light scattering detector. System C consisted of a Waters Alliance 2695 separation module equipped with a Waters 2487 dual-wavelength absorbance detector and an IN/US Systems β-RAM Flow-Through System Model 2 radiochemical detector. For system C, 100% of the eluent flow was diverted to the β-RAM where it was mixed with 2 volumes of In-Flow 2:1 universal liquid scintillator; the dwell time was 0.4 s.

Characterization of PGHS-2 Oxygenation Products of 3-HPAA. Murine PGHS-2 (200 nM) was reconstituted with 2 equiv of heme in 1 mL of reaction buffer at 37 °C for 3 min. Following reconstitution, 3-HPAA was added to the protein to a final concentration of 25 μM, and the reaction was allowed to proceed for 10 min at 37 °C. The reaction was quenched by the addition of ethyl acetate containing 0.5% acetic acid and 25 μM *N*-(3-methoxyphenyl)arachidonylamide as an internal standard (IS). The organic layer was removed and dried under argon gas. The resultant residue was suspended in an acetonitrile/water mixture (1:3). Products were separated on a Luna C18(2) column (10.0 cm × 0.2 cm, 3 μm) using system A or system B. The mobile phase consisted of aqueous 0.5% acetic acid (A) and 0.5% acetic acid in acetonitrile (B). Separation was performed with a flow rate of 0.3 mL/min, holding at 40% B for 2 min before increasing to 100% B over 30 min. The flow was held at 100% B for 15 min prior to a return to starting conditions.

LC−MS and LC−MS/MS were performed using similar conditions on a Waters Alliance 2690 Separation Module coupled to a Thermofinnigan TSQ7000 triple-quadrupole mass spectrometer. Separation was performed with a flow rate of 0.25 mL/min, holding at 40% B for 2 min before increasing to 100% B over 20 min. The flow was held at 100% B for 10 min prior to a return to starting conditions. The instrument was operated in positive ion mode using electrospray ionization with a spray voltage of 4.5 kV and a capillary temperature of 225 °C. Full scan analysis was performed from *m*/*z* 350.00 to 550.00 with a scan rate of 0.5. Ions of interest were selected for CID using a collision energy of −15 eV.

For silver ion coordination ion spray MS (Ag^+CIS-MS) and MS/MS, LC was conducted on a Surveyor Separation Module using a Luna C18(2) column (10.0 cm × 0.2 cm, 3 μm). The mobile phase consisted of aqueous 80 μM silver acetate (A) and 80 μM silver acetate in methanol. Separation was performed at a flow rate of 0.25 mL/min, holding at 75% B for 1 min before increasing to 100% B over 15 min. The flow was held at 100% B for 5 min prior to a return to starting conditions. The instrument was operated in positive ion mode using electrospray ionization with a spray voltage of 3 kV and a capillary temperature of 225 °C. Full scan analysis was performed from *m*/*z* 400.00 to 600.00 with a scan rate of 1.0. Ions of interest were selected for CID using a collision energy of −30 eV.

Characterization of PGHS-1 Oxygenation Products of 3-HPAA. Ovine PGHS-1 (500 nM) was reconstituted with 2 equiv of heme in 2.5 mL of reaction buffer at 37 °C, and reactions were conducted and samples analyzed by LC−MS as described for PGHS-2. Tween 20, a component of PGHS-1 purification, caused ion suppression, which prevented direct detection of 3-HPAA product molecular ions in full scan mode. Ions of products identified in PGHS-2 samples were selected for CID in PGHS-1 samples using a collision energy of −15 eV.

Ovine PGHS-1 (500 nM) or murine PGHS-2 (50 nM) was reconstituted with 2 equiv of heme in a 200 μL reaction mixture and incubated with 25 μM [^{14}C]-3-HPAA for 10 min at 37 °C. Reactions were quenched by the addition of ethyl acetate containing 0.5% acetic acid. Aliquots of the organic layer were spotted on a normal phase thin layer chromatography plate and developed in a mobile phase that was a 75:25:1 ethyl acetate/methylene chloride/acetic acid mixture at 4 °C. These conditions have been previously reported for the separation of arachidonic acid and its products of oxidation by PGHS (*28*). Radiolabeled products and unreacted 3-HPAA were quantified with a radioactivity scanner (Bioscan Inc., Washington, DC). The plate was then exposed to a phosphor screen for approximately 85 h prior to imaging with a Bio-Rad (Hercules, CA) Molecular Imager FX.

Assessment of Covalent Modification of PGHS-2 by 3-HPAA. Covalent modification of PGHS-2 was assessed by adaptation of a previously reported method (*29*). ApoPGHS-2 or

PGHS-2 with 0.5 equiv of hematin (holoPGHS-2) was incubated with 2 or 5 equiv of [^{14}C]-3-HPAA in 100 mM Tris-HCl (pH 8.0) at room temperature. After incubation with [^{14}C]-3-HPAA for 5 min, samples were placed on ice to slow the reaction. LC was achieved on system C with a Vydac Protein C4 column (25.0 cm × 0.46 cm, 5 μm) equipped with a widebore C4 security guard cartridge. The mobile phase was a 9:1 H_2O/ACN mixture with 0.1% trifluoroacetic acid (A) or a 1:9 H_2O/ACN mixture with 0.1% trifluoroacetic acid (B). Separation was performed at a flow rate of 1 mL/min, holding at 40% B for 4 min before increasing to 60% B over 30 min. The flow was held at 60% B for 5 min prior to a return to starting conditions. Protein was detected by absorbance at 280 nm and eluted at 24.4 min. Heme was detected by absorbance at 405 nm and eluted at 6.8 min. [^{14}C]-3-HPAA was detected by absorbance at 280 nm and by radiochemical detection and eluted at 32.2 min.

Assessment of Heme Modification by 3-HPAA. Incubations were set up and separated as described above for assessment of covalent modification of PGHS-2, with the exception that unlabeled 3-HPAA was used in place of [^{14}C]-3-HPAA, and separation was conducted on system A to allow monitoring of the heme absorbance spectrum.

RESULTS

Metabolism of 3-HPAA by PGHS. While investigating the inhibition of PGHS by AM404 analogues using an oxygen uptake assay, we observed no oxygen consumption upon addition of AM404 (up to 50 μM) to PGHS-1 or PGHS-2. In contrast, 3-HPAA was oxygenated by both PGHS-1 and PGHS-2. The rate of oxygen uptake was measured at various concentrations of 3-HPAA and arachidonic acid, and the Michaelis−Menten kinetic parameters were determined (Table 1 and Figure 2). Oxygen uptake rates at 3-HPAA concentrations above 50 μM were not reproducible due to the limited solubility of the compound. The overall efficiency of 3-HPAA metabolism by PGHS-1 was approximately 10-fold lower than that of arachidonic acid, as evidenced by k_{cat}/K_m. The resulting efficiency for 3-HPAA metabolism by PGHS-2 was reduced by less than 3-fold. The k_{cat} values for the two substrates were comparable for PGHS-2, but the K_m for 3-HPAA was higher. In contrast to arachidonate, oxygenation of 3-HPAA by PGHS-2 was significantly inhibited at high substrate concentrations.

Characterization of Products of 3-HPAA Oxidation by PGHS-2. Following incubations of PGHS-2 with 3-HPAA, mixtures were extracted, separated by HPLC, and analyzed using either a diode array detector or a triple-quadrupole mass spectrometer. Eluting components were detected by absorbance at 245 nm, a wavelength characteristic of the phenolamide moiety (Figure 3). No additional products could be detected via evaporative light scattering detection or mass spectrometry. Labeled peaks were not observed in controls lacking either 3-HPA or protein.

UV spectra of products 1−4 closely resemble those of 3-HPA (Figure 4 and Figure S1 of the Supporting Information). Product 1 was not sufficiently resolved via LC−MS to gather mass spectrometric data. Products 2−4 exhibited similar mass spectra, with m/z values of 466, 461, 444, 426, and 408 as major ions (Figure 5A and Figures S2 and S3A of the Supporting Information). $[M + H]^+$ (m/z 444) corresponds to the incorporation of three atoms of oxygen, consistent with a prostaglandin (PG)-derived species. This was supported by Ag^+CIS-MS, in which the major ions observed were at m/z 550 and 552 (Figure S4 of the Supporting Information); these were the predicted ions for a PG-derived species coordinated with $^{107}Ag^+$ and $^{109}Ag^+$, the most abundant naturally occurring isotopes. Under standard LC−MS conditions, other ions present in the spectra represent the ammonium and sodium adducts, m/z 461 and 466, respectively, as well as the neutral loss of one or two waters, m/z 426 and 408 (Figure 5A). Further characterization of products 2 and 4 was achieved by collision-induced dissociation (CID) of m/z 444; due to the low abundance of m/z 444 for product 3, CID did not provide a sufficient signal-to-noise ratio for resolution of specific fragment ions. CID of products 2 and 4 yielded similar fragments, the most prevalent being m/z 426, 408, 317, and 299 (Figure 5B and Figure S3B of the Supporting Information). The

Table 1: Michaelis−Menten Kinetic Parameters for Oxygenation of Arachidonic Acid (AA) and 3-HPAA by PGHS[a]

	PGHS-1		PGHS-2	
	AA	3-HPAA	AA	3-HPAA
k_{cat} (s^{-1})	51 ± 3	22 ± 1	47 ± 2	48 ± 3
K_m (μM)	3.4 ± 0.6	15 ± 1	2.5 ± 0.4	6 ± 1
k_{cat}/K_m (s^{-1} μM^{-1})	15 ± 1	1.5 ± 1	19 ± 1	7 ± 2

[a]Parameters ± the standard deviation were determined by nonlinear regression of data shown in Figure 2.

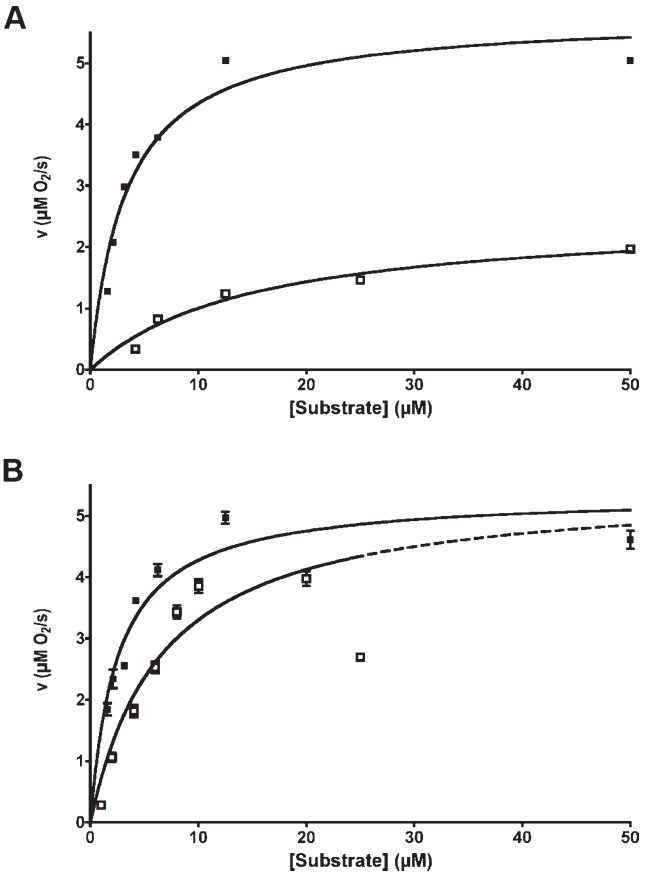

FIGURE 2: Concentration dependence of maximal rates of arachidonate (■) and 3-HPAA (□) oxygenation by (A) PGHS-1 and (B) PGHS-2. Each point represents the mean ± standard deviation of three independent measurements. Kinetic parameters were determined by nonlinear regression and are reported in Table 1. The dashed line in panel B represents the fit predicted in the absence of substrate inhibition.

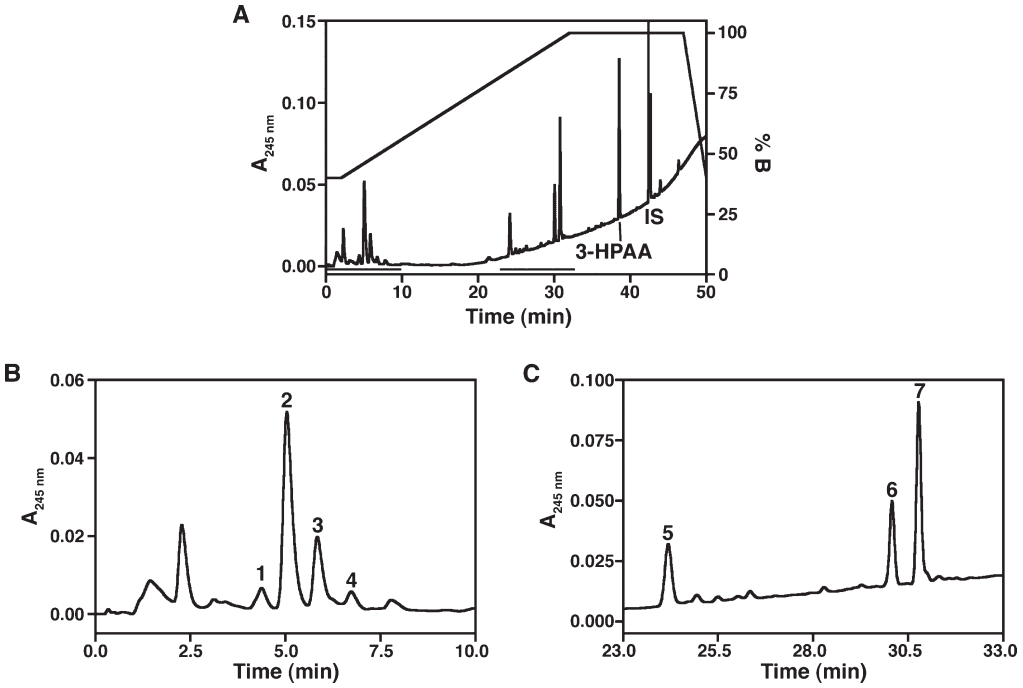

FIGURE 3: Chromatographic profile of products of PGHS-2-dependent oxygenation of 3-HPAA. (A) Following incubation of PGHS-2 with 3-HPAA, products were separated by reverse phase chromatography (elution gradient on the right axis) and eluting products detected via absorbance at 245 nm. Expanded views of the two major sets of products are shown in panels B and C. Labeled peaks were not observed in blank reaction mixtures lacking either PGHS-2 or 3-HPAA. IS denotes internal standard.

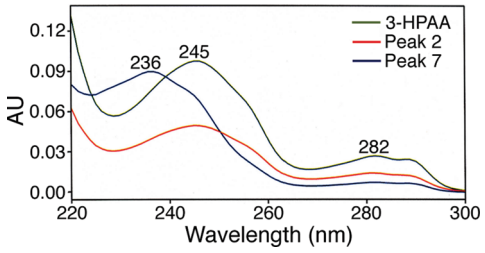

FIGURE 4: UV profiles of 3-HPAA and two products of 3-HPAA oxygenation by PGHS-2. Peak numbers correspond to assignments made in Figure 3. UV profiles of all products of 3-HPAA oxygenation are provided in Figure S1 of the Supporting Information.

full scan Q1 and CID spectra are consistent with PGE_2/D_2-PA, nonenzymatic degradation products of PGH_2-PA (Figure 5C). An authentic standard of PGE_2-PA was synthesized; the HPLC retention time and full scan Q1 and CID spectra were identical to those of product 2 (Figure S5 of the Supporting Information), supporting the hypothesis that this product is PGE_2-PA. PGD_2 differs from PGE_2 only in the position of the carbonyl and hydroxyl on the cyclopentane ring, and CID fragmentation patterns of the isomers are indistinguishable. On reversed phase chromatography systems, PGE_2 elutes before PGD_2, and this elution order is maintained for the glyceryl esters and ethanolamides (unpublished observations). Thus, product 4 likely represents PGD_2-PA. Product 5 exhibits ions at m/z 394, 389, and 354, which may represent adducts of sodium and ammonium and the neutral loss of water from 12-hydroxyheptadecatrienoylphenolamide (HHT-PA), which results from the loss of malonaldehyde from PGH_2-PA (Figure 6). CID of the ion at m/z 389 yields ions at m/z 372 (the presumed $[M + H]^+$), 354 (neutral loss of water), and 244 (loss of aminophenol and water). Taken together, analysis of products 2−5 strongly supports the hypothesis that PGHS-2 produces PG-like products from 3-HPAA.

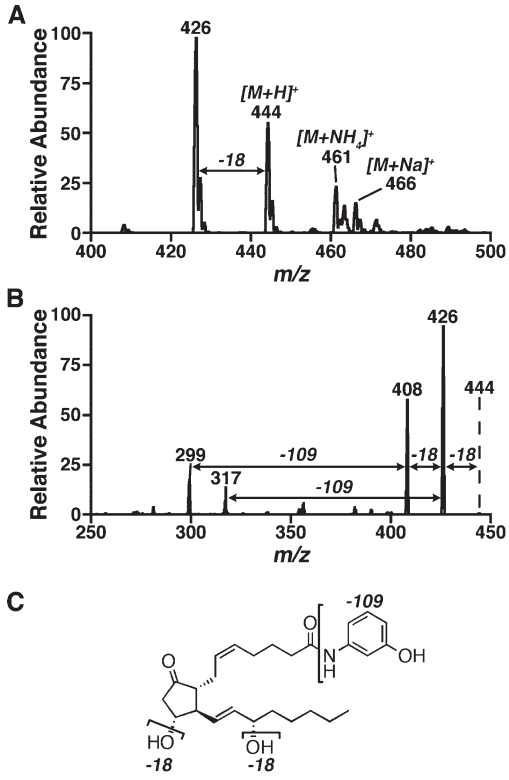

FIGURE 5: Mass spectral characterization and proposed structure of a prostaglandin-like product formed by oxygenation of 3-HPAA by PGHS-2. (A) Full scan MS of peak 2. (B) CID of the ion at m/z 444 at peak 2. (C) Proposed structure and fragmentation of product 2. Loss of hydroxyl groups (17 mu) is observed via CID as a neutral loss of water (18 mu). The structure shown is that of PGE_2-PA.

Products 6 and 7 represent a distinct class of oxygenation products assigned as hydroxyeicosatetranoyl-phenolamides (HETE-PAs). Both products absorbed strongly at 236 nm,

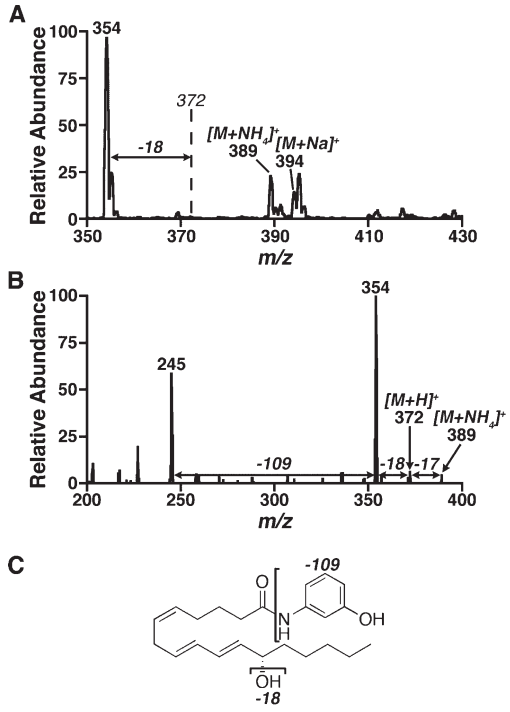

FIGURE 6: Mass spectral characterization and proposed structure of an HHT-like product formed following oxygenation of 3-HPAA by PGHS-2. (A) Full scan MS of peak 5. (B) CID of the ion at *m*/*z* 389 at peak 5, the ammoniated adduct of the ion at *m*/*z* 372. (C) Proposed structure and fragmentation of product 5. Loss of the hydroxyl group (17 mu) is observed via CID as a neutral loss of water (18 mu).

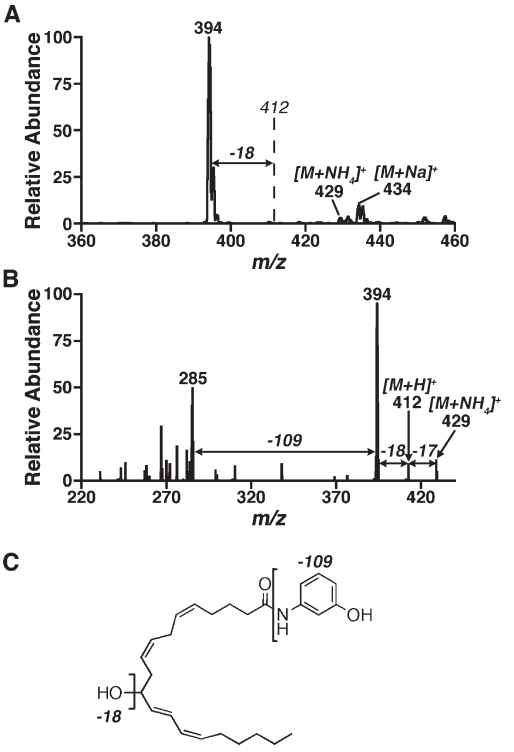

FIGURE 7: Mass spectral characterization and proposed representative structure of a HETE-like product formed following oxygenation of 3-HPAA by PGHS-2. (A) Full scan MS of peak 7. (B) CID of the ion at *m*/*z* 429 at peak 7, the ammoniated adduct of the ion at *m*/*z* 412. (C) Proposed representative structure and fragmentation of product 7. Loss of the hydroxyl group (17 mu) is observed via CID as a neutral loss of water (18 mu). Fragments consistent with a proposed structure of 11-HETE-PA were detected using Ag^+CIS-MS/MS (Figure S6B of the Supporting Information).

characteristic of a conjugated diene system (Figure 4). Full scan Q1 spectra of both products exhibited an ion at *m*/*z* 394 (Figure 7A). This is likely a result of the neutral loss of water from the $[M + H]^+$ species of HETE-PA, which would have an ion at *m*/*z* 412. Small amounts of ions at *m*/*z* 434 and 429 were observed, corresponding to the sodiated and ammoniated molecular ions. Using Ag^+CIS-MS, ions at *m*/*z* 518 and 520 were observed at approximately equal intensities, consistent with $^{107}Ag^+$ and $^{109}Ag^+$ adducts of a mono-oxygenated product of 3-HPAA (Figure S6A of the Supporting Information). CID of the presumed ammonium adduct of product 7 (*m*/*z* 429) yielded fragments corresponding to the loss of water and aminophenol (Figure 7B). However, the signal:noise ratio in the resulting CID spectrum was insufficient to permit assignment of the position of oxygenation. Ag^+CIS-MS/MS of the ion at *m*/*z* 518 revealed distinct fragmentation patterns for products 6 and 7 (Figure S6B, C of the Supporting Information). On the basis of the mechanism of arachidonic acid metabolism by PGHS-2 and fragmentation observed by Ag^+CIS-MS/MS, it is hypothesized that products 6 and 7 represent 15- and 11-HETE-PA, respectively.

Characterization of Products of 3-HPAA Oxidation by PGHS-1. The products of 3-HPAA oxidation by PGHS-1 were analyzed by LC−MS in positive ion mode. However, Tween 20, the detergent used in purification of PGHS-1, caused ion suppression in full scan mode (Figures S7 and S8 of the Supporting Information). CID was conducted for ions at *m*/*z* 444, 389, and 429, the ions of interest identified from PGHS-2 samples. This allowed detection of products in PGHS-1 samples with retention times and CID spectra similar to those of products 2 [PGE_2-PA (Figure S9 of the Supporting Information)] and 5 [HHT-PA (Figure S10 of the Supporting Information)] in PGHS-2 samples. In addition, PGHS was incubated with [^{14}C]-3-HPAA, and the product profiles were compared by TLC. With PGHS-1, the observed products comigrated with PGHS-2 products (Figure 8). Quantification suggested that the distribution of products was similar for PGHS-1 and PGHS-2 (Table S1 of the Supporting Information). However, to achieve a similar extent of 3-HPAA metabolism, the concentration of PGHS-1 required was 10-fold higher than that of PGHS-2. The data indicate that

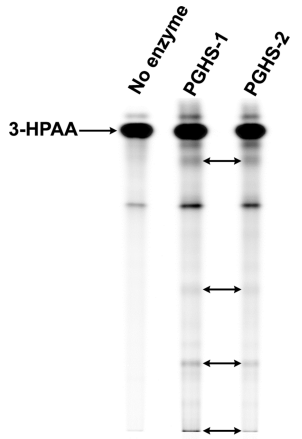

FIGURE 8: Oxygenation of [^{14}C]-3-HPAA by PGHS. [^{14}C]-3-HPAA was incubated in buffer alone or with 500 nM PGHS-1 or 50 nM PGHS-2. Products were analyzed by thin layer chromatography. Spots (indicated by arrows) that were not in controls lacking protein but were observed in PGHS-1 samples comigrate with PGHS-2 products. Radiometric quantification of products is shown in Table S1 of the Supporting Information.

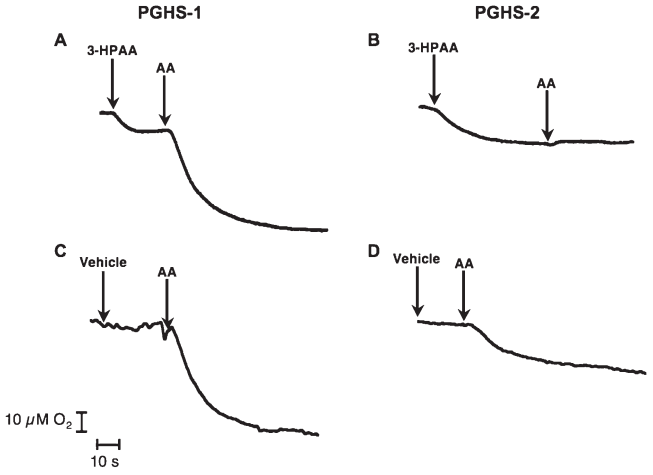

FIGURE 9: Oxygenation of 3-HPAA by PGHS-1 and PGHS-2 and subsequent oxygenation of arachidonic acid. Upon addition of 25 μM 3-HPAA to PGHS-1 (A) or PGHS-2 (B), oxygen in solution was consumed, indicating metabolism of 3-HPAA. Once oxygenation of 3-HPAA had proceeded to completion, 25 μM arachidonic acid (AA) was added. PGHS-1 could still metabolize arachidonate, as evidenced by oxygen consumption, but PGHS-2 was completely inactivated. Control curves for oxygenation of AA following incubation with vehicle are also shown for PGHS-1 (C) and PGHS-2 (D).

PGHS-1 converts 3-HPAA to products similar to PGHS-2, albeit less efficiently.

Inactivation of PGHS by 3-HPAA. At high concentrations of 3-HPAA, the rate of 3-HPAA oxygenation by PGHS-2 was drastically reduced (Figure 2), suggesting the enzyme might be undergoing inactivation. Therefore, the ability of 3-HPAA to inhibit oxidation of arachidonate by PGHS was examined. Following metabolism of 25 μM 3-HPAA, PGHS-1 showed an only 30% reduction in its ability to oxidize arachidonic acid. Because of the low solubility of 3-HPAA at higher concentrations, an IC_{50} for PGHS-1 could not be determined. However, under the same conditions, PGHS-2 was completely inactivated (Figure 9).

To determine the IC_{50}, the concentration of 3-HPAA required to inhibit activity by 50%, PGHS-2 was incubated with 3-HPAA until oxygen uptake was complete or for 30 s, if oxygen uptake was undetectable. Following the preincubation with 3-HPAA, 25 μM arachidonic acid was added, and the rate of oxygenation was determined and normalized to the DMSO control (Figure 10). An IC_{50} of 1.6 μM was determined with complete inactivation occurring at $\geq$10 μM. At concentrations of $<$1 μM, turnover of 3-HPAA was undetectable; at these same concentrations, arachidonic acid metabolism was minimally inhibited. However, significant inactivation of PGHS-2 was observed at concentrations of 3-HPAA corresponding to observable metabolism of 3-HPAA, whereas complete inactivation of PGHS-1 could not be achieved.

To determine if the inactivation of PGHS-2 by 3-HPAA was reversible, holo-PGHS-2 was incubated with 10 μM 3-HPAA, a concentration of 3-HPAA at which no residual enzymatic activity remained. Following incubation with 3-HPAA or vehicle, the protein sample was subjected to ultrafiltration to remove excess inhibitor and analyzed for its ability to metabolize arachidonic acid (Figure S11 of the Supporting Information). The sample treated with 3-HPAA did not metabolize arachidonic acid following ultrafiltration, indicating that inactivation of PGHS-2 by 3-HPAA was irreversible.

Assessment of PGHS-2 Protein and Heme Modification by 3-HPAA. Inactivation of PGHS-2 by 3-HPAA could potentially be mediated by damage to the heme moiety of PGHS-2 or modification of the protein. Following incubation of PGHS-2 with [^{14}C]-3-HPAA, protein samples were analyzed by HPLC with UV and radiochemical detection. Radioactivity did not coelute with either protein or heme, indicating that 3-HPAA did not covalently modify the protein or the heme (Figure S12 of the Supporting Information). PGHS-2 also was incubated with unlabeled 3-HPAA, and samples were analyzed using LC with a photodiode array detector to allow monitoring of the heme spectrum. No change in the retention time or the heme spectrum was noted, indicating that 3-HPAA did not cause oxidative damage to the heme or cross-linking of heme to the protein (Figure S13 of the Supporting Information).

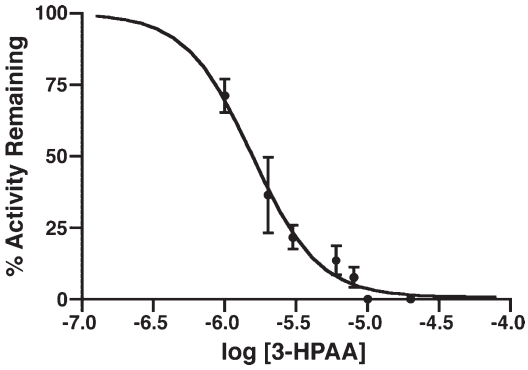

FIGURE 10: Concentration dependence of PGHS-2 inactivation by 3-HPAA. PGHS-2 was incubated with various concentrations of 3-HPAA. Once oxygenation of 3-HPAA had proceeded to completion, arachidonic acid (25 μM) was added. The maximal rate of oxygen uptake was determined and normalized to vehicle control. Each point represents the mean $\pm$ standard deviation of three independent measurements.

DISCUSSION

Oxidation of arachidonic acid by PGHS is critical in numerous physiological and pathophysiological states (*1*, *2*). The growing list of substrates that can be metabolized by PGHS, often selectively by PGHS-2, highlights the importance of characterizing the interaction of fatty acid-derived molecules with lipid dioxygenases, particularly when such compounds, including AM404, are utilized in vivo to study the biology of complex signaling networks. The interactions of *N*-(hydroxyphenyl)-arachidonoylamides with PGHS provide an interesting example of how subtle structural perturbations can significantly impact the binding of small molecule to their targets. The *para* isomer (AM404) acts as an inhibitor of PGHS (*18*), whereas we report here that the *meta* isomer serves as a substrate for PGHS.

3-HPAA is more efficiently metabolized by PGHS-2 than PGHS-1, as observed with many other arachidonoyl amides and esters. For PGHS-2, k_{cat} is identical for arachidonate and 3-HPAA. The higher K_M for 3-HPAA accounts for differences in the catalytic efficiency (k_{cat}/K_M) for 3-HPAA and arachidonate. The efficiency of 3-HPAA oxygenation by PGHS-2 is somewhat surprising, as *N*-arachidonoyldopamine and its *O*-desmethyl analogue are poor substrates for this enzyme (*30*). PGHS-2 produces phenolamide derivatives of prostaglandins and HETEs from 3-HPAA. The same classes of products are observed for arachidonic acid and 2-arachidonoylglycerol, suggesting 3-HPAA adopts a conformation similar to that of other arachidonoyl derivatives. Although PGHS-1 oxidizes 3-HPAA much

less efficiently than PGHS-2, PGHS-1 seems to produce a similar product profile.

Following metabolism of 3-HPAA, oxygenase activity is reduced in both PGHS-1 and PGHS-2. PGHS-1 activity is reduced by only 30% at 25 μM 3-HPAA, whereas PGHS-2 is completely and irreversibly inactivated. Metabolism of 3-HPAA does not seem to result in covalent modification, oxidation, or cross-linking of the heme moiety. In addition, covalent modification of PGHS-2 protein was not detectable. This behavior is quite similar to substrate-dependent autoinactivation of PGHS, which is observed with arachidonate and other substrates. The mechanism of PGHS autoinactivation remains elusive. As with 3-HPAA, inactivation during arachidonate turnover is not associated with heme inactivation (*31*, *32*). Covalent modification of PGHS has been observed following metabolism of arachidonate, but this occurs on a time scale slower than that of autoinactivation (*33*−*35*). A favored model of autoinactivation suggests that a critical residue such as the catalytic tyrosine, Tyr-385, is damaged during the course of catalysis. Oxidative damage to PGHS may provide a mechanism for inactivation of PGHS by 3-HPAA as well. Oxidation of side chains has not previously been reported for PGHS, although this may be due to inadequate technology for assessing such modifications, which would produce a mass shift of only 1, 2, or 16 mass units.

N-(Hydroxyphenyl)arachidonoylamides provide a unique series for elucidating determinants of binding of ligands to PGHS. A definitive switch from inhibitor to substrate is noted by moving the hydroxyl group from the *para* to the *meta* position on the phenyl ring. This suggests that 3-HPAA adopts a distinct conformation that permits it to be oxygenated by PGHS. Future structural studies of the *para* and *meta* isomers bound to PGHS could provide unique insights into the structural determinants of ligand binding and metabolism.

ACKNOWLEDGMENT

Molecular graphics were produced using the UCSF Chimera package from the Resource for Biocomputing, Visualization, and Informatics at the University of California, San Francisco (supported by National Institutes of Health Grant P41 RR-01081) (*36*). We thank Samir Saleh for assistance with the synthesis of PGE_2-PA.

SUPPORTING INFORMATION AVAILABLE

Thirteen figures (Figures S1−S13) and one table (Table S1). This material is available free of charge via the Internet at http://pubs.acs.org.

REFERENCES

1. Dubois, R. N., Abramson, S. B., Crofford, L., Gupta, R. A., Simon, L. S., Putte, L. B., and Lipsky, P. E. (1998) Cyclooxygenase in biology and disease. *FASEB J. 12*, 1063–1073.
2. Vane, J. R., Bakhle, Y. S., and Botting, R. M. (1998) Cyclooxygenases 1 and 2. *Annu. Rev. Pharmacol. Toxicol. 38*, 97–120.
3. O'Banion, M. K., Winn, V. D., and Young, D. A. (1992) cDNA cloning and functional activity of a glucocorticoid-regulated inflammatory cyclooxygenase. *Proc. Natl. Acad. Sci. U.S.A. 89*, 4888–4892.
4. Xie, W. L., Chipman, J. G., Robertson, D. L., Erikson, R. L., and Simmons, D. L. (1991) Expression of a mitogen-responsive gene encoding prostaglandin synthase is regulated by mRNA splicing. *Proc. Natl. Acad. Sci. U.S.A. 88*, 2692–2696.
5. Hla, T., and Neilson, K. (1992) Human cyclooxygenase-2 cDNA. *Proc. Natl. Acad. Sci. U.S.A. 89*, 7384–7388.
6. Seibert, K., Zhang, Y., Leahy, K., Hauser, S., Masferrer, J., Perkins, W., Lee, L., and Isakson, P. (1994) Pharmacological and biochemical demonstration of the role of cyclooxygenase 2 in inflammation and pain. *Proc. Natl. Acad. Sci. U.S.A. 91*, 12013–12017.
7. Kurumbail, R. G., Stevens, A. M., Gierse, J. K., McDonald, J. J., Stegeman, R. A., Pak, J. Y., Gildehaus, D., Miyashiro, J. M., Penning, T. D., Seibert, K., Isakson, P. C., and Stallings, W. C. (1996) Structural basis for selective inhibition of cyclooxygenase-2 by anti-inflammatory agents. *Nature 384*, 644–648.
8. Rowlinson, S. W., Crews, B. C., Lanzo, C. A., and Marnett, L. J. (1999) The binding of arachidonic acid in the cyclooxygenase active site of mouse prostaglandin endoperoxide synthase-2 (COX-2). A putative L-shaped binding conformation utilizing the top channel region. *J. Biol. Chem. 274*, 23305–23310.
9. Malkowski, M. G., Ginell, S. L., Smith, W. L., and Garavito, R. M. (2000) The productive conformation of arachidonic acid bound to prostaglandin synthase. *Science 289*, 1933–1937.
10. Kozak, K. R., Prusakiewicz, J. J., Rowlinson, S. W., Prudhomme, D. R., and Marnett, L. J. (2003) Amino acid determinants in cyclooxygenase-2 oxygenation of the endocannabinoid anandamide. *Biochemistry 42*, 9041–9049.
11. Kozak, K. R., Prusakiewicz, J. J., Rowlinson, S. W., Schneider, C., and Marnett, L. J. (2001) Amino acid determinants in cyclooxygenase-2 oxygenation of the endocannabinoid 2-arachidonylglycerol. *J. Biol. Chem. 276*, 30072–30077.
12. Marnett, L. J., and Maddipati, K. R. (1991) Peroxidases in chemistry and biology , Vol. 1, CRC Press, Boca Raton, FL.
13. Rieke, C. J., Mulichak, A. M., Garavito, R. M., and Smith, W. L. (1999) The role of arginine 120 of human prostaglandin endoperoxide H synthase-2 in the interaction with fatty acid substrates and inhibitors. *J. Biol. Chem. 274*, 17109–17114.
14. Luong, C., Miller, A., Barnett, J., Chow, J., Ramesha, C., and Browner, M. F. (1996) Flexibility of the NSAID binding site in the structure of human cyclooxygenase-2. *Nat. Struct. Biol. 3*, 927–933.
15. Kozak, K. R., Rowlinson, S. W., and Marnett, L. J. (2000) Oxygenation of the endocannabinoid, 2-arachidonylglycerol, to glyceryl prostaglandins by cyclooxygenase-2. *J. Biol. Chem. 275*, 33744–33749.
16. Wada, M., DeLong, C. J., Hong, Y. H., Rieke, C. J., Song, I., Sidhu, R. S., Yuan, C., Warnock, M., Schmaier, A. H., Yokoyama, C., Smyth, E. M., Wilson, S. J., FitzGerald, G. A., Garavito, R. M., Sui, D. X., Regan, J. W., and Smith, W. L. (2007) Enzymes and Receptors of Prostaglandin Pathways with Arachidonic Acid-derived Versus Eicosapentaenoic Acid-derived Substrates and Products. *J. Biol. Chem. 282*, 22254–22266.
17. Yu, M., Ives, D., and Ramesha, C. S. (1997) Synthesis of prostaglandin E2 ethanolamide from anandamide by cyclooxygenase-2. *J. Biol. Chem. 272*, 21181–21186.
18. Hogestatt, E. D., Jonsson, B. A., Ermund, A., Andersson, D. A., Bjork, H., Alexander, J. P., Cravatt, B. F., Basbaum, A. I., and Zygmunt, P. M. (2005) Conversion of acetaminophen to the bioactive N-acylphenolamine AM404 via fatty acid amide hydrolase-dependent arachidonic acid conjugation in the nervous system. *J. Biol. Chem. 280*, 31405–31412.
19. Piomelli, D., Beltramo, M., Glasnapp, S., Lin, S. Y., Goutopoulos, A., Xie, X. Q., and Makriyannis, A. (1999) Structural determinants for recognition and translocation by the anandamide transporter. *Proc. Natl. Acad. Sci. U.S.A. 96*, 5802–5807.
20. Lastres-Becker, I., de Miguel, R., De Petrocellis, L., Makriyannis, A., Di Marzo, V., and Fernandez-Ruiz, J. (2003) Compounds acting at the endocannabinoid and/or endovanilloid systems reduce hyperkinesia in a rat model of Huntington's disease. *J. Neurochem. 84*, 1097–1109.
21. Costa, B., Siniscalco, D., Trovato, A. E., Comelli, F., Sotgiu, M. L., Colleoni, M., Maione, S., Rossi, F., and Giagnoni, G. (2006) AM404, an inhibitor of anandamide uptake, prevents pain behaviour and modulates cytokine and apoptotic pathways in a rat model of neuropathic pain. *Br. J. Pharmacol. 148*, 1022–1032.
22. La Rana, G., Russo, R., D'Agostino, G., Sasso, O., Raso, G. M., Iacono, A., Meli, R., Piomelli, D., and Calignano, A. (2008) AM404, an anandamide transport inhibitor, reduces plasma extravasation in a model of neuropathic pain in rat: Role for cannabinoid receptors. *Neuropharmacology 54*, 521–529.
23. Glaser, S. T., Abumrad, N. A., Fatade, F., Kaczocha, M., Studholme, K. M., and Deutsch, D. G. (2003) Evidence against the presence of an anandamide transporter. *Proc. Natl. Acad. Sci. U.S.A. 100*, 4269–4274.
24. Yue, H.-Y., Fujita, T., Kawasaki, Y., and Kumamoto, E. (2004) AM404 enhances the spontaneous release of α-glutamate in a manner sensitive to capsazepine in adult rat substantia gelatinosa neurones. *Brain Res. 1018*, 283–287.
25. Marnett, L. J., Siedlik, P. H., Ochs, R. C., Pagels, W. R., Das, M., Honn, K. V., Warnock, R. H., Tainer, B. E., and Eling, T. E. (1984)

Mechanism of the stimulation of prostaglandin H synthase and prostacyclin synthase by the antithrombotic and antimetastatic agent, nafazatrom. *Mol. Pharmacol. 26*, 328–335.
26. Turman, M. V., Kingsley, P. J., Rouzer, C. A., Cravatt, B. F., and Marnett, L. J. (2008) Oxidative metabolism of a fatty acid amide hydrolase-regulated lipid, arachidonoyltaurine. *Biochemistry 47*, 3917–3925.
27. Misra, H. P., and Fridovich, I. (1976) A convenient calibration of the Clark oxygen electrode. *Anal. Biochem. 70*, 632–634.
28. Kalgutkar, A. S., Crews, B. C., Rowlinson, S. W., Garner, C., Seibert, K., and Marnett, L. J. (1998) Aspirin-like Molecules that Covalently Inactivate Cyclooxygenase-2. *Science 280*, 1268–1270.
29. Chen, Y. N., Bienkowski, M. J., and Marnett, L. J. (1987) Controlled tryptic digestion of prostaglandin H synthase. Characterization of protein fragments and enhanced rate of proteolysis of oxidatively inactivated enzyme. *J. Biol. Chem. 262*, 16892–16899.
30. Prusakiewicz, J. J., Turman, M. V., Vila, A., Ball, H. L., Al-Mestarihi, A. H., Marzo, V. D., and Marnett, L. J. (2007) Oxidative metabolism of lipoamino acids and vanilloids by lipoxygenases and cyclooxygenases. *Arch. Biochem. Biophys. 464*, 260–268.
31. Hemler, M. E., Graff, G., and Lands, W. E. (1978) Accelerative autoactivation of prostaglandin biosynthesis by PGG2. *Biochem. Biophys. Res. Commun. 85*, 1325–1331.
32. Hemler, M. E., and Lands, W. E. (1980) Evidence for a peroxide-initiated free radical mechanism of prostaglandin biosynthesis. *J. Biol. Chem. 255*, 6253–6261.
33. Boutaud, O., Brame, C. J., Chaurand, P., Li, J., Rowlinson, S. W., Crews, B. C., Ji, C., Marnett, L. J., Caprioli, R. M., Roberts, L. J.II, and Oates, J. A. (2001) Characterization of the lysyl adducts of prostaglandin H-synthases that are derived from oxygenation of arachidonic acid. *Biochemistry 40*, 6948–6955.
34. Kulmacz, R. J. (1987) Attachment of substrate metabolite to prostaglandin H synthase upon reaction with arachidonic acid. *Biochem. Biophys. Res. Commun. 148*, 539–545.
35. Eling, T. E., Wilson, A. G., Chaudhari, A., and Anderson, M. W. (1977) Covalent binding of an intermediate(s) in prostaglandin biosynthesis to guinea pig lung microsomal protein. *Life Sci. 21*, 245–251.
36. Pettersen, E. F., Goddard, T. D., Huang, C. C., Couch, G. S., Greenblatt, D. M., Meng, E. C., and Ferrin, T. E. (2004) UCSF Chimera: A visualization system for exploratory research and analysis. *J. Comput. Chem. 25*, 1605–1612.